



HAL
open science

Determination of the mechanical properties of gelatinized starch granule from bulk suspension characterization

Arnesh Palanisamy, Gabrielle Moulin, Marco Ramaioli, Artemio Plana-Fattori, Denis Flick, Paul Menut

► **To cite this version:**

Arnesh Palanisamy, Gabrielle Moulin, Marco Ramaioli, Artemio Plana-Fattori, Denis Flick, et al.. Determination of the mechanical properties of gelatinized starch granule from bulk suspension characterization. *Rheologica Acta*, 2022, 10.1007/s00397-022-01325-4 . hal-03626461

HAL Id: hal-03626461

<https://hal.science/hal-03626461v1>

Submitted on 31 Mar 2022

HAL is a multi-disciplinary open access archive for the deposit and dissemination of scientific research documents, whether they are published or not. The documents may come from teaching and research institutions in France or abroad, or from public or private research centers.

L'archive ouverte pluridisciplinaire **HAL**, est destinée au dépôt et à la diffusion de documents scientifiques de niveau recherche, publiés ou non, émanant des établissements d'enseignement et de recherche français ou étrangers, des laboratoires publics ou privés.

Determination of the mechanical properties of gelatinized starch granule from bulk suspension characterization

Arnesh Palanisamy^a, Gabrielle Moulin^a, Marco Ramaioli^a, Artemio Plana-Fattori^a, Denis Flick^a, Paul Menu^t^{a,*}

^a*Université Paris Saclay, INRAE, AgroParisTech, UMR SayFood, 91300, Massy, France*

Abstract

Gelatinized starch granules are soft and deformable particles that are commonly used in food products as texture modifiers. Modelling the flow behaviour of such suspensions during industrial processes requires the knowledge of the mechanical properties of the swollen granules, however, such data is usually lacking because of the difficulties inherent to the determination of mechanical properties of particles that are heterogeneous in terms of size and shape. We investigate here the rheological properties of dense suspensions prepared at different volume fractions and by different means (centrifugation, limited water swelling, osmotic compression) to estimate the mechanical properties of an "averaged" starch granule. Results show that starch granule exhibits a rough surface and behave as frictional particles. We compare the shear modulus value determined assuming either frictionless (previous model) or frictional interactions (as suggested by our results), the latter giving shear modulus lower by about one order of magnitude. This study also allows the first estimate of the starch granule bulk modulus, which value is corresponding to a Poisson ratio of 0.47, close to the maximum value of 0.5. The swollen granule shear modulus is also shown to be temperature independent in the range commonly found in industrial processes (20-90 °C). These results pave the way towards multiscale mechanistic modelling of the flow of starch suspensions, to derive macroscopic rheological properties from the description of the microscopic granule properties.

Keywords: Microgel, Shear modulus, Bulk modulus, Thermal effects, Particle Elasticity

1. Introduction

In its native form, starch is found as dense granules in a variety of grains and tubers. After industrial fractionation and in some cases, chemical/thermal treatments, a large variety of starch granules with contrasted properties are obtained. These starch granules that differ in terms of textural properties, or stability against mechanical, Physico-chemical or thermal stresses, are produced for various specific applications such as enhanced oil recovery in oil drilling applications or thickening agents in food products (Ratnayake and Jackson, 2008; Nawaz et al., 2020). Global starch production is expected to reach around 156 metric tonnes by 2025 (Reportlinker.com, 2020), of this roughly 60% is used for food-based applications and 40% is expected to be used for industrial uses including oil, pharmaceutical, paper, etc.

Thermal treatments are commonly used in food processing and are usually applied to products that are highly hydrated. Applying a thermal treatment to native starch granules in the presence of excess water results in important modifications of their properties. In their native state, starch granules are solid particles, more or less spherical, in which starch macromolecules (amylopectin and amylose) are densely packed so that these granules only have a very limited water absorption capacity. However, if the temperature exceeded $\sim 70^\circ\text{C}$, an important swelling of the particles is very rapidly observed if water is available around the granule. The influx of water is driven by the enthalpic interactions between the hydrogen bonding sites of starch and water (Renzetti et al., 2021). This process, during which the particle can absorb more than 10 times its mass in water, is called gelatinization. During gelatinization, the volume fraction of the starch particles present in a starch suspension strongly increases, and so does the suspension viscosity.

If the volume fraction of the particles in solution remains very low, i.e. much below the random close packing volume fraction ϕ_{rcp} , that is the maximum volume fraction that can be reached by solid undeformable particles packed randomly, it behaves as a hard particle suspension at low shear rates (Einstein, 1905; Batchelor, 1977). However, at high enough starch volume fractions, these suspensions form thick pastes (gelatinization is also called

*corresponding author

Email address: paul.menut@agroparistech.fr (Paul Menut)

28 starch pasting(Chen et al., 2007)) which exhibit properties that are similar to the ones
29 of dense suspensions of soft microgel particles, with both solid-like and fluid-like proper-
30 ties(Seth et al., 2006). At low stresses, they behave like elastic solids and deform reversibly
31 under stress. However, once sufficient stress is reached they begin to flow and show the
32 properties of a fluid. The threshold stress at which they begin to flow is called the yield
33 point. Soft particle pastes have a jammed amorphous microstructure that is the source of
34 their rheological behaviour. At volume fractions higher than ϕ_{rcp} , soft particles start to
35 deform to accommodate more neighbouring particles (Menut et al., 2012; de Aguiar et al.,
36 2018). Further compression results in particle shrinkage. Therefore, their volume fraction,
37 also called packing fraction, that is estimated from the volume occupied by the particles in
38 the diluted state, can exceed 1 (Seth et al., 2006; Evans and Lips, 1992).

39 With the advent of particle-based simulation methods, such as Discrete Element Mod-
40 elling and CFD-DEM, there is significant interest in developing simple methods to charac-
41 terize material properties such as particle Young’s modulus and Poisson’s ratio, required as
42 a model input. One of the most common contact models used for simulating particles is
43 the Hertzian contact model. This model takes into account the curvature of the spherical
44 surfaces while predicting the interaction forces on the colliding particles. According to this
45 contact model, a repulsive force exists when the granules overlap and no force exists when
46 they do not overlap (Di Renzo and Di Maio, 2005). To predict these normal and tangential
47 repulsive forces one needs two parameters namely, Young’s modulus and Poisson’s ratio.
48 To fully describe suspensions behaviour, lubrication forces need to be integrated, they arise
49 due to the presence of the fluid layers in between particles. The momentum of a granule
50 is imparted to the surrounding fluid and subsequently the other granules, hence leading to
51 transport of momentum, even when granules are not physically in contact with each other.
52 One requires interstitial fluid viscosity, surface roughness, position and velocities of particles
53 for predicting the lubrication forces. For homogeneous isotropic materials, simple relations
54 exist between the three elastic constants are Young’s modulus, the bulk modulus and the
55 shear modulus. These relations allow calculating them all as long as two are known, as they
56 are related by the following equations.

$$K = \frac{E}{3(1 - 2\nu)} \quad (1)$$

$$G = \frac{E}{2(1 + \nu)} \quad (2)$$

57 where K , G , E and ν are respectively the bulk modulus, shear modulus, Young’s mod-
58 ulus and Poisson’s ratio. These relations could be applied to describe the whole behaviour
59 of dense suspensions, which at a macroscopic scale could be considered homogeneous and
60 isotropic. Individual starch granules, however, are non-spherical particles, and their in-
61 dividual behaviour might deviate significantly from one of the homogeneous and isotropic
62 particles. Therefore a strategy could be to determine only “averaged” properties, as it is usu-
63 ally done for example for their size determination, done by static light scattering assuming
64 a spherical shape.

65 Techniques at the particle level exists for deciphering materials properties of individ-
66 ual particle material properties in literature (Villone et al., 2019; Villone and Stone, 2020;
67 Abate et al., 2012; Mohapatra et al., 2017). Typical techniques include atomic force mi-
68 croscopy(AFM) based on nano-indentation, Brillouin light scattering(BLS), microfluidics,
69 tensionmeter. In AFM based techniques a Poisson ratio is assumed and the Young’s modulus
70 is deducted from resisting force vs displacement data (Kaufman et al., 2017; Aufderhorst-
71 Roberts et al., 2018). However, these techniques are not straightforward to apply to measure
72 a particle averaged modulus for such a complex system of soft particles with a very high
73 degree of variability in terms of size and shapes. BLS data is used to infer the Poisson’s
74 ratio (Mohapatra et al., 2017). In microfluidic approaches, a particle is compressed through
75 a tapered channel and as pressure is developed by increasing the flow rate, the particle de-
76 forms due to the pressure and penetrates further into the channel. The penetration depth
77 is optically observed and Young’s modulus is deduced (Villone et al., 2019). Similarly, ten-
78 sionmeter and microgel based techniques make use of surface tension to generate force for
79 deformation and optical techniques for measuring the deformation (Abate et al., 2012; Vil-
80 lone and Stone, 2020). However, the applicability of these techniques is not straightforward

81 for non-spherical, poly-disperse, complex suspensions such as starch suspensions. Typical
82 DEM models make the spherical particle assumption, albeit the ‘multi-sphere’ approach and
83 methods for specific shapes such as super-quadratics exists (Lane et al., 2010; Preece et al.,
84 1999). For non-spherical particles with no particular shape features, it is a standard practice
85 to simulate spherical particles with averaged particle properties. One simple methodology to
86 obtain such average particle properties is to infer them from the bulk response of the dense
87 suspensions, which behave macroscopically as homogeneous isotropic materials, and then to
88 determine from that an ”averaged” properties at the level of the individual particles. Such
89 use of average ‘calibration techniques’ are also a common feature in powder and dry granu-
90 lar material simulations using DEM (He et al., 2015; Yan et al., 2016; Orefice and Khinast,
91 2020). This approach is also useful in ‘coarse-graining’ simulations where the actual system
92 is too large and one simulates at a mesoscale with larger ‘representative particles’ instead of
93 actual particle sizes to reduce the computational costs.

94 In this article, the average mechanical properties of a large population of starch granules
95 are investigated from bulk rheological measurements conducted on dense suspensions. To
96 estimate the average particle shear modulus, the suspension shear modulus was measured
97 . Two extreme hypothesis were considered, namely the fully frictional and the friction-less
98 scenarios, to determine an upper and a lower limit for the particle shear modulus. The
99 likelihood of the two assumptions is critically discussed. Then, we investigate the particles
100 bulk modulus by osmotic compression. Finally, we investigate how particles shear modulus
101 depend on the temperature, in the range 20-90°C.

102 **2. Materials and methods**

103 Chemically cross-linked waxy maize starch (C*Tex 06205), provided by Cargil (Bauppte,
104 France) was used for the entire study. Waxy maize starch contains more than 99 % amy-
105 lopectin, and chemical cross-linking prevents the release of macromolecules during gelatiniza-
106 tion.

107 *2.1. True density measurement*

108 The starch particles true density was measured using an air pycnometer (micromeritics
109 AccuPyc 1330). We determined a true density $\rho_{true, starch} = 1.321 \pm 0.002$ g/ml (average
110 value from 6 repeats).

111 *2.2. Centrifugation*

112 In a 2-litre mixing vessel, we introduced 15 grams of starch before the addition of 1 litre
113 of distilled water. The mixture was heated to 90 °C while mixing a 50 rpm using an IKA
114 eurostar 60 mixer with a 3 blade propeller of diameter 5 cm; and held at this temperature for
115 15 minutes to ensure complete swelling of the starch granules. After letting the suspension
116 cool down to room temperature, it was transferred into centrifuge tubes and centrifuged
117 (SIGMA 3-18KS centrifuge) in the required conditions of rotation speed and duration. The
118 supernatant (excess water layer) was carefully removed and the pellet, which consisted of
119 densely packed swollen starch granules, was recovered for rheological characterization and
120 dry weight measurements to estimate the volume fraction. A combination of centrifugation
121 speeds ranging from 500g to 10000g and centrifugation duration ranging from 15 minutes
122 to 30 minutes resulted in swollen starch suspensions with volume fractions ϕ ranging from
123 0.447 to 0.552.

124 *2.3. Osmotic compression*

125 22.5 grams of starch were added to 1.5 l of distilled water in a mixing vessel. The mixture
126 was gelatinized at 90 °C as described previously (2.2). After letting the suspension cool
127 down to room temperature, it was transferred into a regenerated cellulose dialysis tube with
128 a cut-off of 6-8 kDa (spectra/por 1, diameter 40 mm). The dialysis tube was clipped at both
129 ends and placed for osmotic compression inside a solution of Poly-Ethylene Glycol (PEG,
130 $20\text{kg}\cdot\text{mol}^{-1}$) of known concentration. After osmotic compression, the compressed samples
131 were recovered and subjected to rheological characterization and dry weight measurements
132 to estimate their volume fraction. We used PEG 20kDa concentrations ranging from 0.2%
133 to 5% (wt/wt) and compression times ranging from 2 to 15 days to produce samples with
134 volume fractions ϕ ranging from 0.46 to 1.69.

135 For the estimation of bulk modulus, we used the same protocol as described above,
136 however, to ensure a constant osmotic pressure (that could decrease with time due to water
137 diffusion from the sample to the PEG bath), the PEG bath was renewed 3 times. To
138 determine the osmotic pressure corresponding to a given PEG concentration, we used the
139 phenomenological one-parameter equation of state proposed by Cohen et al. (2009), which
140 correctly described the behaviour of PEG (and others neutral flexible polymers in good
141 solvents). This equation, based on the sum of a van 't Hoff and a des Cloizeaux terms, include
142 a fitted parameter α , also called the “crossover index”, which is polymer size-dependent and
143 for which we used the value proposed by Li et al. (2015) for PEG 20kDa. In that case, the
144 osmotic compression lasted around 17 days to ensure equilibrium without any degradation
145 or granule softening.

146 *2.4. Limited water swelling*

147 After the addition of a known quantity of starch (ranging from 5 to 25 grams) into
148 100ml of water in a mixing vessel, the suspension was heated up to 90 °C and held at this
149 temperature for 15 min under constant mixing. The sample was then cooled down to room
150 temperature and recovered for rheological characterization and dry weight measurements.
151 This resulted in starch suspension with volume fractions ϕ ranging from 0.42 to 1.90.

152 *2.5. Dry weight measurement and volume fraction determination*

153 Dry weight measurements were conducted at 100 °C in an oven (Chopin technologies).
154 Prior measurements showed that after 24h at 100 °C the sample had reached a constant
155 weight, therefore all samples were let in the oven for 24h before dry weight measurement.
156 Samples were introduced in an aluminium foil previously weighted, and the weight of the
157 sample was determined before (M_1) and after (M_2) drying so that the sample dry starch
158 content could be determined as $S_{dry} = M_2/M_1$. Therefore, the starch concentration in the
159 suspension, C_s (in g of starch per 100g of water) is given by $C_s = 100 * \frac{S_{dry}}{1-S_{dry}}$

160 The corresponding equivalent volume fraction of unswollen starch granules, ϕ_{ug} , is given by

$$\phi_{ug} = \frac{C_s}{\rho_{true,starch}} * \frac{1}{100 + \frac{C_s}{\rho_{true,starch}}} \quad (3)$$

161 With $\rho_{true,starch}$ the true density of unswollen starch previously determined assuming density
162 for water $\rho_{water} = 1000 \text{ kg/m}^3$.

163 To estimate the volume fraction of swollen granules, we used data from previous micro-
164 scopic experiments showing that, on average, the starch granule radius (the geometric mean
165 of the Feret diameters) increases 2.35 times when gelatinized in excess of water (Palanisamy
166 et al., 2020; Deslandes et al., 2019). Thus, assuming that the granules are spherical and the
167 total volume is conserved (volume gained by the starch during swelling is lost by water),
168 one can estimate the volume of the swollen starch granules divided by the volume of the
169 suspension: ϕ , which is also known as the volume fraction. Please note that based on the
170 definition here volume fraction is notional and thus can exceed 1. Similar definitions have
171 been used extensively in the literature for various other suspensions as well (Mattsson et al.,
172 2009).

$$\phi = (2.35^3) * \phi_{ug} \quad (4)$$

173 2.6. Rheology

174 The rheological measurements were all performed in a Couette cell using an Anton Paar
175 MCR92 rheometer. The characterization of the dense suspensions of swollen starch granules
176 was performed at 20 °C. The mechanical properties were first probed at constant frequency
177 ($f = 1 \text{ Hz}$) and strain ($\gamma = 0.01$) for 120 seconds, with an acquisition rate of 1 point per
178 second. Then, a frequency sweep was carried out at constant strain $\gamma = 0.01$, from $f = 0.02$
179 Hz to $f = 3.5 \text{ Hz}$. Storage modulus obtained from single point measurements are plotted in
180 figure 1. The frequency and loading effects were negligible compared to the volume effects.

181 The effect of temperature on the rheological properties was also evaluated. A rejuve-
182 nation and ageing step was performed prior to the first measurement, in order to limit

183 measurements error resulting from the sample history (Cloitre et al. (2000)). Rejuvenation
184 consists of shearing the sample at shear stress greater than the yield stress thus allowing
185 the flow of the sample. Here, the sample was sheared at a shear rate $\dot{\gamma} = 50 \text{ s}^{-1}$. The
186 following ageing step consists in holding the sample at rest for 45 minutes. Sedimentation
187 experiments showed the absence of settling in the sample during all the duration of the
188 experiments, which can be attributed to the large volume fraction of the samples (above
189 random loose packing), combined with a low density difference between the swollen starch
190 granules and the surrounding water. Rheological properties were measured at 20 °C; 40 °C,
191 60 °C, 80 °C and finally 90 °C, the ramp rate during heating being 2 °C per minute. At
192 each temperature, the rheological properties were measured at constant frequency $f = 1 \text{ Hz}$
193 and constant strain $\gamma = 0.01$ for 120 seconds with an acquisition rate of 1 point per second.
194 For cooling the sample from 90 °C to 20 °C, a ramp rate of 0.4 °C per minute was used, and
195 sample properties were again measured once thermal equilibrium was reached.

196 *2.7. Confocal laser scanning microscopy*

197 Gelatinized samples obtained by the limited water swelling method and characterized
198 by a particle volume fraction close to 0.4 were observed using a confocal laser scanning
199 microscope (CLSM) (Leica TCS SP8, Germany). 0.5 ml of starch solution was stained using
200 50 μL of Congo Red solution (1% in water, Sigma-Aldrich). Two 250 μm thick spacers were
201 used to place the stained solutions on the microscope slides. The solutions were excited
202 with a laser at 488 nm and the emitted fluorescence was detected in the range 497 - 717 nm.
203 The laser was used at 85% of the maximum intensity. Samples were observed with a 40X
204 water objective. The total number of pixels in each picture is 3224 x 3224 and each pixel
205 correspond to 0.09 μm . Thus, the length and width of each picture corresponds to 290.62
206 μm . A total of 192 scans were performed using 0.422 μm step for a total sample height of
207 80.67 μm to generate a stack of images. Each of these 192 images was manually analyzed
208 to count the number of neighbours of some representative granules.

209 *2.8. Bulk modulus measurements through osmotic compression*

210 To measure the bulk modulus of the suspension using osmotic compression, one first needs
 211 to establish the time taken for the sample to equilibrate osmotically with the surrounding
 212 medium. To do so, we followed the dry weight evolution during osmotic compression, at two
 213 different PEG concentrations, and determined the corresponding volume fraction (Table 1).
 214 After 17 days, the volume fraction tend to reach a plateau. Above 17 days, the increase
 215 in volume fraction is very limited, but we observed by rheology a decrease in the sample
 216 shear modulus, that could result from starch degradation and granule softening, thus only
 217 samples obtained after 17 days will be considered for analysis.

| time [days] | ϕ -3% PEG20K [wt/wt] | ϕ -4% PEG20K [wt/wt] |
|-------------|---------------------------|---------------------------|
| 4 | 0.76 | 0.99 |
| 9 | 1.20 | 1.60 |
| 14 | 1.39 | 1.67 |
| 17 | 1.45 | 1.69 |
| 21 | 1.46 | 1.75 |
| 24 | 1.47 | 1.75 |

Table 1: Evolution of the sample volume fraction during osmotic compression, at two different PEG concentrations

218 **3. Results and Discussion**

219 *3.1. Suspension rheology and estimation of the particle shear modulus*

220 We observed that starting from $\phi \sim 0.4$, suspensions exhibit a finite value of elastic mod-
 221 ulus. By contrast to what is observed in colloidal systems, which are liquid till the random
 222 closed packing, suspensions of granular particles can exhibit a finite modulus at volumes
 223 fractions much lower, due to the formation of a self-supporting stress-bearing network. The
 224 minimum volume fraction at which this network can form is called the random loose packing,
 225 its value depends on the shape but also the frictional properties of the particles(Silbert, 2010;
 226 Dong et al., 2006). Starting from the random loose packing, the shear modulus (measured
 227 at $f = 1\text{Hz}$ and $\gamma = 0.01$) of dense suspensions of swollen starch granules strongly increases
 228 with volume fraction, as illustrated in figure 1. Whatever the method used to prepare dense

229 suspensions, namely centrifugation, osmotic compression or limited water swelling, the data
 230 superimposed. Whatever the history associated with each procedure, the final stage that
 231 is reached is reproducible in terms of rheological characterization and the granule volume
 232 fraction is the key parameter that controls the elastic behaviour of the paste. Even in the
 233 case of limited water swelling, for which granule never reached their full swelling capacity
 234 due to the limited amount of water (for $\phi > 1$), the properties of the suspension are identical
 235 to the one of fully swollen starch granules that were partially dehydrated by compression.
 236 Two regimes are observed concerning the elastic modulus dependency toward volume frac-
 237 tion. First, from above the random loose packing to $\phi \approx 0.7$, the shear modulus strongly
 238 increases with the volume fraction. Then, a transition zone exists for $0.7 < \phi < 1$. For
 239 volume fraction $\phi > 1$, the dependence of shear modulus on volume fraction is much weaker.
 240 Insert in Figure 1 shows the log-log plot which shows the existence of the two regimes and
 241 the power law dependence of shear modulus with the notional volume fraction of granules.
 242 Fitting a power law to these regimes resulted in the following equation

$$G' = \begin{cases} 1600\phi^{3.15} & 0.4 \leq \phi \leq 0.7 \\ 550\phi^{0.53} & 1 \leq \phi \end{cases}$$

243 A similar increase in shear modulus with notional volume fraction have been reported
 244 by Evans and Lips (1990); Abdulmola et al. (1996); Rodriguez-Hernandez et al. (2006). The
 245 existence of two regimes of shear modulus with volume fraction for swollen starch suspensions
 246 is reported in Evans and Lips (1992). Also, for comparison Evans and Lips (1992) reported
 247 values of suspension shear modulus around 750 Pa and 1000 Pa at notional volume fraction
 248 of 1, for two different grades of chemically modified maize starches.

249 Whatever the volume fraction, the elastic modulus of the suspension only show a very
 250 weak dependency on the frequency. This is illustrated in the insert of figure 1 for 3 different
 251 volume fractions achieved via 3 sample preparation methods, in the first, intermediate and
 252 second regime. As reported by Seth et al. (2006), soft particle suspension moduli are function
 253 of the frequency. Seth et al. (2006) even predicted from simulations G_0 and G_∞ (storage

254 moduli at low and high frequency). We show from the following data that the relationship
 255 of storage moduli with frequency are similar across the volume fractions tested.

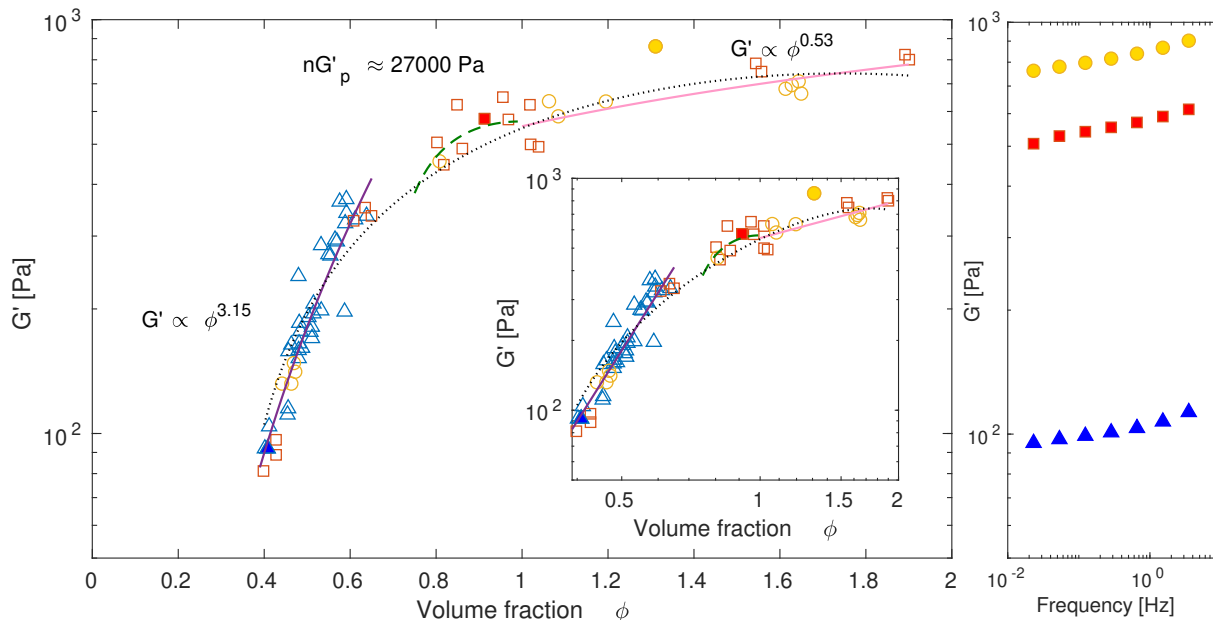


Figure 1: Suspension shear modulus as a function of volume fraction. Triangles[Δ], Squares[\square], circles[\circ] represent samples prepared via centrifugation, limited water swelling and osmotic compression respectively ($\gamma = 0.01$, $f = 1$ Hz). The solid dotted line represents the polynomial fit of overall experimental data ($G_{suspension} = -352\phi^2 + 1229\phi - 330$). The purple continuous line represents the power-law fit for volume fractions $\phi < \phi_{rcp}$, Green dashed line represents the best fit from the Evans and Lips (1990) model for $0.8 < \phi < 1$, Pink continuous line represents the power law fit for volume fractions $\phi > 1$. *Insert*: The same figure in the log-log plot.

Right-side plot: Dependence on frequency: volume fraction of three samples prepared via centrifugation, limited water swelling and osmotic compression correspond to 0.4, 0.91, 1.31.

256 For friction-less systems, Evans and Lips (1990) derived an analytical equation that links
 257 the suspension shear modulus with the individual granule shear modulus and the average
 258 number of neighbouring granules. This model assumes a Hertzian potential (contact model)
 259 between granules. The equation, valid for $\phi_{rcp} < \phi < 1$, is as follows:

$$G'_{susp} = \frac{\phi_{rcp} n G'_p}{5\pi(1-\nu)} \left(\left(\frac{\phi}{\phi_{rcp}} \right)^{\frac{1}{3}} \left(1 - \left(\frac{\phi}{\phi_{rcp}} \right)^{-\frac{1}{3}} \right)^{\frac{1}{2}} - \frac{8}{3} \left(\frac{\phi}{\phi_{rcp}} \right)^{\frac{2}{3}} \left(1 - \left(\frac{\phi}{\phi_{rcp}} \right)^{-\frac{1}{3}} \right)^{\frac{3}{2}} \right) \quad (5)$$

260 where G'_{susp} is the suspension shear modulus, ϕ_{rcp} is the volume fraction at random close

261 packing and n is the average number of neighbouring granules respectively.

262 Given a granule size distribution one can estimate the ϕ_{rcp} based on the relationship
263 proposed by Farr and Groot (2009) as previously done in Shewan and Stokes (2015a,b);
264 Shewan et al. (2021). In the system investigated, the size distribution of Feret diameters
265 of swollen starch granules has been previously determined, it is characterized by a normal
266 distribution with mean = 33.1 μm and standard deviation = 10.7 μm . With this value, $\phi_{rcp} =$
267 0.68 was determined. The average number of neighbours for each granule, n , was estimated
268 using confocal microscopy. This method was previously used for PMMA spheres by van der
269 Vaart et al. (2013) and also allowed to measure the pair correlation function. In fact, they
270 predicted suspension shear moduli at high frequency with Young's modulus obtained from
271 atomic force microscopy and pair correlation function from confocal microscopy.

272 In figure 1 we show the fit of equation 5 for the truncated data in the volume fraction
273 range of $\phi_{rcp} < \phi < 1$. As we can see from equation 5, G_p depends on the assumption of
274 the average coordination number n of each granule. To determine n , confocal images were
275 acquired on suspensions and the coordination number of 10 different granules was manually
276 counted for each of them, based on the contacts that were observed in different layers.

277 Figure 2 shows the confocal cross-section image of the starch granule suspension at
278 $\phi = 0.4$, the maximum fraction that could be reached for which each granule could still be
279 easily distinguished from its neighbours. Here, $\phi < \phi_{rcp}$ and n could depend on ϕ (van
280 Hecke, 2009), the value determined at this volume fraction might differ from the one at
281 $\phi = 1$, that should be used to apply the Evans and Lips model. Experimental studies have
282 shown that once particles are in contact, further compression first result in a decrease in the
283 void fraction de Aguiar et al. (2018) and local deformation at the contact point de Aguiar
284 et al. (2017). As a result, the increase in coordination number with volume fraction might be
285 limited, especially if friction is present in the system. From the image acquired by confocal
286 microscopy, it is evident that the starch granules are far from being spherical. It should be
287 noted that if the granule seems hollow, this is likely due to the fact that dye (congo red) is
288 adsorbed only on the surface of the granule. In figure 2 we tracked one selected granule from
289 its base (top-left image) to its top (bottom-right image). For this selected granule 5 contacts

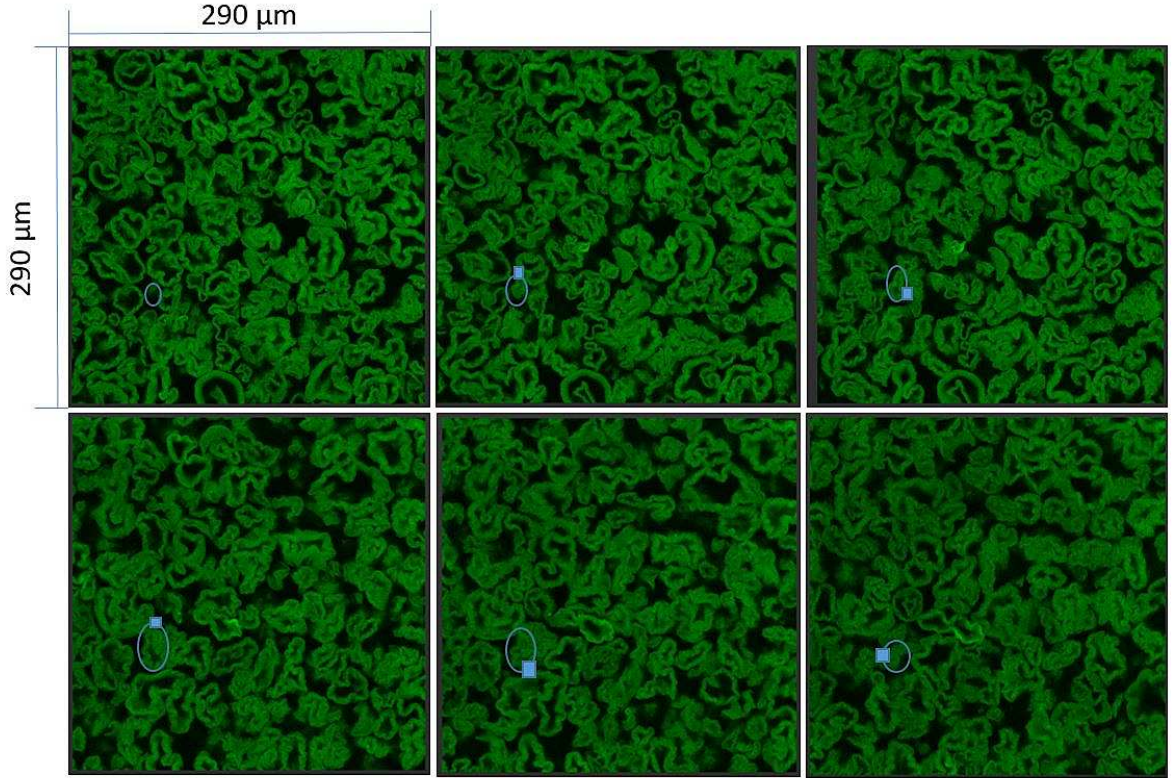


Figure 2: Confocal stack images of starch granule suspension.
 Blue Boxes (\square) correspond to the contact of the traced granule with the neighbouring granule.

290 were observed with neighbouring granules (highlighted as blue boxes on the pictures). This
 291 analysis was carried out to analyze ten different granules, for which we found coordination
 292 numbers varying from 5 (min) to 8 (max).

293 Therefore, with $n = (5,8)$ and a Poisson's ratio $\nu = 0.5$, values obtained for the particle
 294 modulus were between $G_p \approx 5300$ Pa and $G_p \approx 3300$ Pa.

295 However, as seen in the confocal images, the particles are far from being spherical and
 296 have hair-like protrusions on the surface. This suggests that friction might be present in the
 297 system, which is coherent with the measure of a finite shear modulus at low volume fraction,
 298 the hallmark of the system above random loose packing concentration. Assuming a fully
 299 frictional case, $G_p \approx G_{suspension}$ at ϕ around 1, and we obtain $G_p \approx 550$ Pa.

300 *3.2. Estimation of particle bulk modulus*

301 To estimate the starch granule bulk modulus, we used osmotic compression experiments
 302 as previously done by de Aguiar et al. (2017) on model microgels. In general terms, the
 303 isotropic compressibility of material of volume V under a pressure P is measured by its bulk
 304 elastic modulus $K = -V \frac{dP}{dV}$. In this study, we do not measure directly the volume of the
 305 sample, but instead, we determined ϕ , which is directly proportional to the sample volume
 306 through the relation $\phi = n_p V_d / V$, where n_p is the particle's number in the sample, V_d is the
 307 average volume of a fully swollen starch granule in the diluted state, and V the volume of
 308 the entire suspension. The bulk modulus of a gelatinized starch paste, compressed under an
 309 osmotic pressure π , can then be written as $K = -(1/\phi) \frac{d\pi}{d(1/\phi)}$, or in a more simple way

$$K = \phi \frac{d\pi_{in}}{d\phi} \quad (6)$$

310 where π , ϕ are the applied osmotic pressure and the starch particle volume fraction in the
 311 suspension respectively. In our experiments, the osmotic pressure is directly linked to the
 312 PEG content in the water bath, so that osmotic pressures ranging from about 18 kPa to
 313 about 19 kPa were experimentally reached (Table 2)

| PEG conc [wt %] | Osmotic pressure [kPa] | Volume fraction(ϕ) [%] |
|-----------------|------------------------|-------------------------------|
| 1 | 1.8 | 77 |
| 1.5 | 3.4 | 99 |
| 2 | 5.4 | 120 |
| 2.5 | 8.0 | 139 |
| 3 | 11.0 | 145 |
| 3.5 | 14.7 | 158 |
| 4 | 18.9 | 169 |

Table 2: Equilibrium osmotic pressure and volume fractions

314 Using equation 6, the estimates for bulk modulus at different volume fraction are shown
 315 in figure 3. Consistently with Nikolov et al. (2020) a linear relationship between suspension
 316 bulk modulus and volume fraction is obtained. The linear trend also agrees well with
 317 the experimental results of Liétor-Santos et al. (2011) for microgel particles comprising
 318 vinyl pyridine and divinyl benzene. Nikolov et al. (2020) showed that suspension bulk

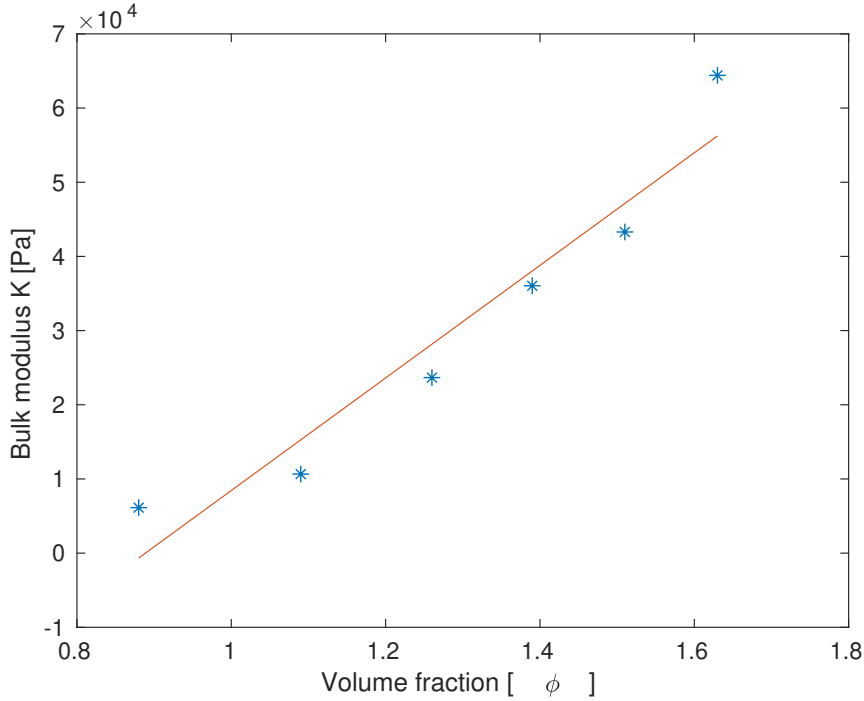


Figure 3: Suspension bulk modulus as function of volume fraction. Asterisks[*] correspond to experimental data.

319 modulus at $\phi = 1$ is roughly equal to $0.8 \times$ particle bulk modulus, and that the ratio of the
 320 suspension bulk modulus to the particle bulk modulus is independent of volume fraction for
 321 $\phi > 1$. From the linear fit in figure 3, it appears that the bulk modulus of the suspension
 322 is about 8.4 kPa at $\phi = 1$. Therefore, an estimate for our starch particle bulk modulus
 323 is $K_{particle} \approx 10.5$ kPa. Using this estimate for bulk modulus and shear modulus of the
 324 suspension at $\phi = 1$, we obtain a Poisson's ratio of 0.47, which is close to the maximum
 325 value of 0.5. By contrast, a Poisson's ratio of 0.33 is obtained if it is calculated using the
 326 friction-less spherical particle assumption. Poisson's ratio for hydrogels reported in literature
 327 ranged from 0.38 to 0.5 (Mohapatra et al., 2017; Boon and Schurtenberger, 2017). This
 328 methodology to characterize the modulus of particles is complementary to the techniques
 329 such as nano-indentation, AFM, etc (Kaufman et al., 2017; Aufderhorst-Roberts et al., 2018).
 330 Such existing alternative techniques are not straightforward to apply to measure a particle
 331 averaged modulus for such a complex system of soft particles with a very high degree of

332 variability in terms of size and shapes.

333 *3.3. Suspension material properties with temperature*

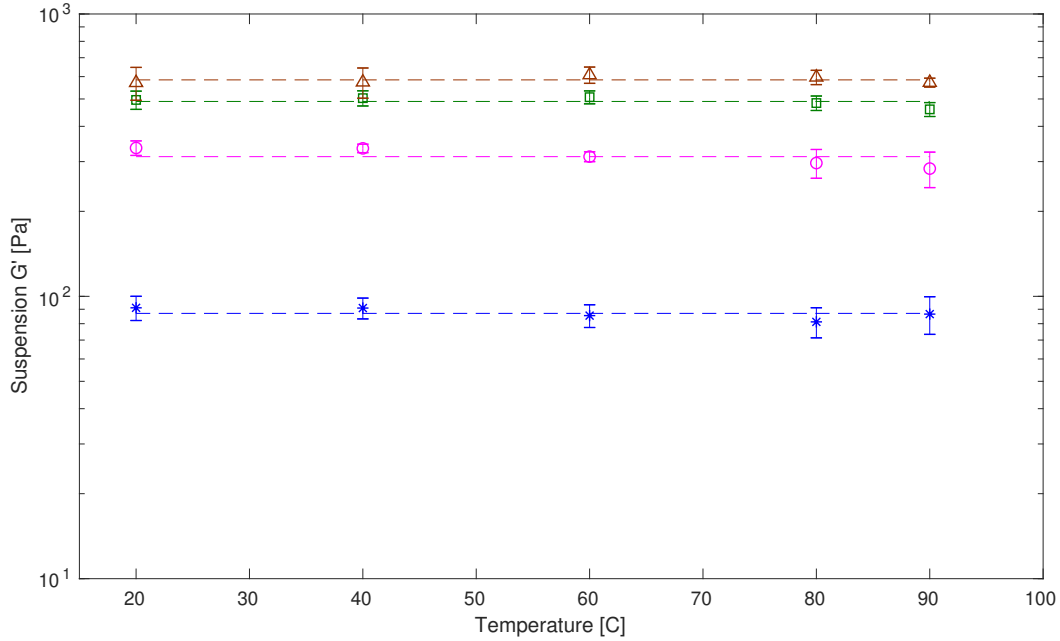


Figure 4: Storage modulus at different temperatures. Asterisks[*], circles[○], boxes[□] and triangles[△] correspond to volume fractions ϕ of 0.42, 0.63, 0.83 and 1.03 respectively. Error bars correspond to one standard deviation. The dashed line is the mean value of all the measurements across temperatures.

334 The storage modulus of the suspension was measured at five different temperatures for
335 four different volume fractions. No significant dependence of shear modulus with temper-
336 ature was observed in the range of temperatures tested. In figure 4 the dotted line is the
337 mean of the measurements of storage moduli at all temperatures for a given volume fraction.
338 These dotted lines fall within the error bars for all volume fractions except for $\phi = 0.63$ at
339 40 °C. Thus, we conclude that the starch granule material properties are independent of
340 the temperature for the tested range of 20 °C to 90 °C. Such temperature independence of
341 hydrogels is also observed by Jing et al. (2021) for polyvinyl alcohol (PVA), carrageenan
342 and calcium-chloride based particles as long as there is no phase change such as melting.

343 3.4. Conclusion

344 This study focused on the rheological properties of fully gelatinized chemically modi-
345 fied waxy maize starch. We characterized suspension shear modulus and suspension bulk
346 modulus at different particles volume fractions, which was reached thanks to three different
347 and independent techniques: centrifugation of a diluted suspension, osmotic compression
348 of a diluted suspension, and controlled swelling of the granules with a limited amount of
349 water. These different techniques allowed to reach a large range of volume fractions but also
350 gave coherent results showing the results are not technique-dependant. The shear and bulk
351 moduli were determined by rheometry and osmotic compression, respectively. From these
352 macroscopic measurements, we estimated the mechanical properties of an “averaged” swollen
353 granule. We first discussed the equation previously used by Evans and Lips (1990), which
354 can be used to estimate the particle shear modulus from the suspension shear modulus, and
355 required an estimate of the average number of neighbouring granules. This was roughly
356 estimated manually using the layered scans of confocal microscopy. Besides Evans and Lips
357 (1990) equation is only valid for perfectly spherical friction-less spheres, which is rarely the
358 case in naturally occurring systems such as starch suspensions, this approach could give an
359 upper bound for the particle shear modulus which was estimated to be around 4400 Pa for
360 this starch. For the lower bound, we considered frictional interactions so that the particle
361 shear modulus is nearly identical to the suspension shear modulus at a volume fraction close
362 to 1. From this assumption, an estimate of particle modulus of 550 Pa was obtained. It
363 seems reasonable, notably in view of the ‘roughness’ of the observed granules to consider
364 rather the second hypothesis. Therefore, assuming frictional interactions, the bulk modulus
365 of the particle was estimated to be around 10.5 kPa. Interestingly, the suspension shear
366 modulus, measured at different volume fractions, were found to be independent of temper-
367 ature, which strongly suggests that starch granules mechanical properties are temperature
368 independent in the range of temperature investigated here. Finally, in a first approach, for
369 this kind of starch, in a fully swollen state, Young’s modulus and Poisson’s ratio of the
370 granules are approximately 1.8 kPa and 0.47 respectively. These estimates could find use in
371 research using modelling and simulation techniques such as DEM and CFD-DEM which in

372 turn help in designing process equipment, process intensification, optimization and design-
373 ing model-based process control. This methodology can be applied to estimate properties of
374 similar microgel systems and of different grades of chemically modified waxy maize starches.

375 4. Acknowledgments

376 This research has been carried out with funding from European Union as part of EU
377 RESEARCH FRAMEWORK PROGRAMME: H2020 / Marie Skłodowska-Curie Actions
378 ITN MATHEGRAM [813202].

379 References

- 380 A. R. Abate, L. Han, L. Jin, Z. Suo, and D. A. Weitz. Measuring the elastic modulus of microgels using
381 microdrops. *Soft Matter*, 8(39):10032–10035, 2012.
- 382 N. Abdulmola, M. Hember, R. Richardson, and E. Morris. Effect of xanthan on the small-deformation
383 rheology of crosslinked and uncrosslinked waxy maize starch. *Carbohydrate Polymers*, 31(1-2):65–78,
384 1996.
- 385 A. Aufderhorst-Roberts, D. Baker, R. J. Foster, O. Cayre, J. Mattsson, and S. D. Connell. Nanoscale
386 mechanics of microgel particles. *Nanoscale*, 10(34):16050–16061, 2018.
- 387 G. Batchelor. The effect of brownian motion on the bulk stress in a suspension of spherical particles. *Journal*
388 *of Fluid Mechanics*, 83(1):97–117, 1977.
- 389 N. Boon and P. Schurtenberger. Swelling of micro-hydrogels with a crosslinker gradient. *Physical Chemistry*
390 *Chemical Physics*, 19(35):23740–23746, 2017.
- 391 G. Chen, O. H. Campanella, and S. Purkayastha. A dynamic model of crosslinked corn starch granules
392 swelling during thermal processing. *Journal of Food Engineering*, 81(2):500–507, 2007.
- 393 M. Cloitre, R. Borrega, and L. Leibler. Rheological aging and rejuvenation in microgel pastes. *Physical*
394 *Review Letters*, 85(22):4819, 2000.
- 395 J. Cohen, R. Podgornik, P. L. Hansen, and V. Parsegian. A phenomenological one-parameter equation of
396 state for osmotic pressures of peg and other neutral flexible polymers in good solvents. *The Journal of*
397 *Physical Chemistry B*, 113(12):3709–3714, 2009.
- 398 I. B. de Aguiar, T. Van de Laar, M. Meireles, A. Bouchoux, J. Sprakel, and K. Schroën. Deswelling and
399 deformation of microgels in concentrated packings. *Scientific Reports*, 7(1):1–11, 2017.
- 400 I. B. de Aguiar, K. Schroën, M. Meireles, and A. Bouchoux. Compressive resistance of granular-scale
401 microgels: From loose to dense packing. *Colloids and Surfaces A: Physicochemical and Engineering*
402 *Aspects*, 553:406–416, 2018.

403 F. Deslandes, A. Plana-Fattori, G. Almeida, G. Moulin, C. Doursat, and D. Flick. Estimation of individual
404 starch granule swelling under hydro-thermal treatment. *Food Structure*, 22:100125, 2019.

405 A. Di Renzo and F. P. Di Maio. An improved integral non-linear model for the contact of particles in distinct
406 element simulations. *Chemical engineering science*, 60(5):1303–1312, 2005.

407 K. Dong, R. Yang, R. Zou, and A. Yu. Role of interparticle forces in the formation of random loose packing.
408 *Physical review letters*, 96(14):145505, 2006.

409 A. Einstein. *Eine neue bestimmung der moleküldimensionen*. PhD thesis, ETH Zurich, 1905.

410 I. Evans and A. Lips. Viscoelasticity of gelatinized starch dispersions. *Journal of Texture Studies*, 23(1):
411 69–86, 1992.

412 I. D. Evans and A. Lips. Concentration dependence of the linear elastic behaviour of model microgel
413 dispersions. *Journal of the Chemical Society, Faraday Transactions*, 86(20):3413–3417, 1990.

414 R. S. Farr and R. D. Groot. Close packing density of polydisperse hard spheres. *The Journal of chemical
415 physics*, 131(24):244104, 2009.

416 Y. He, Z. Wang, T. Evans, A. Yu, and R. Yang. Dem study of the mechanical strength of iron ore compacts.
417 *International Journal of Mineral Processing*, 142:73–81, 2015.

418 H. Jing, J. Shi, P. Guoab, S. Guan, H. Fu, and W. Cui. Hydrogels based on physically cross-linked network
419 with high mechanical property and recasting ability. *Colloids and Surfaces A: Physicochemical and
420 Engineering Aspects*, 611:125805, 2021.

421 G. Kaufman, S. Mukhopadhyay, Y. Rokhlenko, S. Nejati, R. Boltyanskiy, Y. Choo, M. Loewenberg, and
422 C. O. Osuji. Highly stiff yet elastic microcapsules incorporating cellulose nanofibrils. *Soft Matter*, 13(15):
423 2733–2737, 2017.

424 J. E. Lane, P. T. Metzger, and R. A. Wilkinson. A review of discrete element method (dem) particle shapes
425 and size distributions for lunar soil. *NASA STI*, 2010.

426 J. Li, M. Turesson, C. A. Haglund, B. Cabane, and M. Skepö. Equation of state of peg/peo in good solvent.
427 comparison between a one-parameter eos and experiments. *Polymer*, 80:205–213, 2015.

428 J. J. Liétor-Santos, B. Sierra-Martín, and A. Fernández-Nieves. Bulk and shear moduli of compressed
429 microgel suspensions. *Physical Review E*, 84(6):060402, 2011.

430 J. Mattsson, H. M. Wyss, A. Fernandez-Nieves, K. Miyazaki, Z. Hu, D. R. Reichman, and D. A. Weitz. Soft
431 colloids make strong glasses. *Nature*, 462(7269):83–86, 2009.

432 P. Menut, S. Seiffert, J. Sprakel, and D. A. Weitz. Does size matter? elasticity of compressed suspensions
433 of colloidal-and granular-scale microgels. *Soft Matter*, 8(1):156–164, 2012.

434 H. Mohapatra, T. M. Kruger, T. I. Lansakara, A. V. Tivanski, and L. L. Stevens. Core and surface microgel
435 mechanics are differentially sensitive to alternative crosslinking concentrations. *Soft matter*, 13(34):5684–
436 5695, 2017.

437 H. Nawaz, R. Waheed, M. Nawaz, and D. Shahwar. Physical and chemical modifications in starch structure
438 and reactivity. *Chemical properties of starch*, page 13, 2020.

439 S. V. Nikolov, A. Fernandez-Nieves, and A. Alexeev. Behavior and mechanics of dense microgel suspensions.
440 *Proceedings of the National Academy of Sciences*, 117(44):27096–27103, 2020.

441 L. Orefice and J. G. Khinast. A novel framework for a rational, fully-automatised calibration routine for
442 dem models of cohesive powders. *Powder Technology*, 361:687–703, 2020.

443 A. Palanisamy, F. Deslandes, M. Ramaioli, P. Menut, A. Plana-Fattori, and D. Flick. Kinetic modelling of
444 individual starch granules swelling. *Food Structure*, page 100150, 2020.

445 D. S. Preece, R. P. Jensen, E. D. Perkins, J. R. Williams, et al. Sand production modeling using superquadric
446 discrete elements and coupling of fluid flow and particle motion. In *Vail Rocks 1999, The 37th US*
447 *Symposium on Rock Mechanics (USRMS)*. American Rock Mechanics Association, 1999.

448 W. S. Ratnayake and D. S. Jackson. Starch gelatinization. *Advances in Food and Nutrition Research*, 55:
449 221–268, 2008.

450 S. Renzetti, I. A. van den Hoek, and R. G. van der Sman. Mechanisms controlling wheat starch gelatinization
451 and pasting behaviour in presence of sugars and sugar replacers: Role of hydrogen bonding and plasticizer
452 molar volume. *Food Hydrocolloids*, 119:106880, 2021.

453 Reportlinker.com. Global starch industry. *GLOBE NEWSWIRE, New York*, 2020.

454 A. Rodriguez-Hernandez, S. Durand, C. Garnier, A. Tecante, and J. L. Doublier. Rheology-structure prop-
455 erties of waxy maize starch–gellan mixtures. *Food Hydrocolloids*, 20(8):1223–1230, 2006.

456 J. R. Seth, M. Cloitre, and R. T. Bonnecaze. Elastic properties of soft particle pastes. *Journal of rheology*,
457 50(3):353–376, 2006.

458 H. M. Shewan and J. R. Stokes. Analytically predicting the viscosity of hard sphere suspensions from the
459 particle size distribution. *Journal of Non-Newtonian Fluid Mechanics*, 222:72–81, 2015a.

460 H. M. Shewan and J. R. Stokes. Viscosity of soft spherical micro-hydrogel suspensions. *Journal of colloid*
461 *and interface science*, 442:75–81, 2015b.

462 H. M. Shewan, G. E. Yakubov, M. R. Bonilla, and J. R. Stokes. Viscoelasticity of non-colloidal hydrogel
463 particle suspensions at the liquid–solid transition. *Soft Matter*, 17(19):5073–5083, 2021.

464 L. E. Silbert. Jamming of frictional spheres and random loose packing. *Soft Matter*, 6(13):2918–2924, 2010.

465 K. van der Vaart, Y. Rahmani, R. Zargar, Z. Hu, D. Bonn, and P. Schall. Rheology of concentrated soft
466 and hard-sphere suspensions. *Journal of Rheology*, 57(4):1195–1209, 2013.

467 M. van Hecke. Jamming of soft particles: geometry, mechanics, scaling and isostaticity. *Journal of Physics:*
468 *Condensed Matter*, 22(3):033101, 2009.

469 M. M. Villone and H. A. Stone. Rotating tensiometer for the measurement of the elastic modulus of
470 deformable particles. *Physical Review Fluids*, 5(8):083606, 2020.

- 471 M. M. Villone, J. K. Nunes, Y. Li, H. A. Stone, and P. L. Maffettone. Design of a microfluidic device for
472 the measurement of the elastic modulus of deformable particles. *Soft matter*, 15(5):880–889, 2019.
- 473 Z. Yan, S. K. Wilkinson, E. H. Stitt, and M. Marigo. Investigating mixing and segregation using discrete
474 element modelling (dem) in the freeman ft4 rheometer. *International journal of pharmaceutics*, 513(1-2):
475 38–48, 2016.